Comparison of the Electronic Conduction Mechanism in MnOx-CaO-SiO2 and FeOx-CaO-SiO2 Slag Systems

Michael Pomeroy,[1] **Glendon Brown,**[1] **Mansoor Barati**[2] **and Kenneth S. Coley**[1,*]

[1] Steel Research Centre, Department of Materials Science and Engineering, McMaster University, Hamilton, Canada

[2] Department of Materials Science and Engineering, University of Toronto

Abstract. The electrical and electronic and ionic transference numbers were measured for slags in the system MnO-CaO-SiO2 using the stepped potential chronoamperometry method. Transference numbers were measured over a range of oxygen partial pressure to evaluate the effect of MnO-CaO-SiO2. The data were compared with previously measured data for the FeO-CaO-SiO2 system. Data were found to fit well, the Diffusion Assisted Hopping Model for electronic conduction previously develop in the authors' laboratory. The only adjustable parameter employed in fitting the data to this model, was, r^*, the maximum spacing at which hopping can occur. A single value for this parameter was used for all manganese data. The value of r^* obtained for the MnO-CaO-SiO2 system was slightly smaller than that for the FeO-CaO-SiO2 system which is in keeping with the relative magnitude of the third ionization energies for Fe and Mn.

Keywords. Slags, electronic conductivity, transference number, manganese.

PACS®(2010). 72.1Eb, 72.60.+g, 72.80.Ph, 72.20Ee, 66.10.Ed.

1 Introduction

Several studies have been carried out on various slag melts, including: FeO-CaO-SiO2 [1], FeO-MnO-SiO2[2], and PbO-SiO2[3]. The study of the electrical conductivites of slags has certainly not been limited to these examples.

* **Corresponding author:** Kenneth S. Coley, Department of Materials Science and Engineering, McMaster University, Steel Research Centre,1280 Main St West, Hamilton, Ontario L8S 4L7, Canada; E-mail: coleyk@mcmaster.ca.

Turkdogan [4] summarizes data from a number of studies of liquid oxides, binary melts and tertiary melts.

In studying FeOx-SiO2 melts, Pastukhov et al. [5] suggest that the ionic conductivity is independent of oxygen potential and that the electronic conductivity can be expressed in terms of oxygen potential:

$$\sigma_e = k p_{O_2}^m,$$
(1)

with m being between 0.11 and 0.14.

Engell and Vygen [6] suggest that the ionic conductivity is dependent upon the oxidation state of the slag:

$$\sigma_i = \sigma_0 - ay,$$
(2)

where σ_0 and a are constants and y represents the ratio of Fe^{3+} to all iron species, Fe_{total}. The electronic conductivity was found to vary according to Equation 3

$$\sigma_e = by(1 - y).$$
(3)

Fontana et al. [7] found that the ionic conductivity in FeO containing melts could be expressed as:

$$\sigma_i = c_1 [Fe_{2+}],$$
(4)

and that the electronic conductivity could be expressed as

$$\sigma_e = c_2 [Fe_{3+}],$$
(5)

where c_1 and c_2 are adjustable coefficients.

Segers et al. cite8 determined the total conductivity of CaO-SiO2-MnO slags for various compositions under inert gas atmospheres. In that study, the total conductivity for the system was found to follow an Arrhenius form for temperatures above the liquidus:

$$\sigma = k \exp\left(\frac{-E_a}{RT}\right).$$
(6)

Jiao and Themelis [9] provide an insightful summary of previous work regarding total slag conductivity, including for the system SiO2-CaO-MgO-MnO. Their work implies that conductivity varies as a linear function of slag basicity and follows an Arrhenius form as a function of temperature. Based the work by Segers et al. [8], Jiao and Themelis developed the following expression for variation of conductivity with slag basicity in the CaO-MgO-MnO-SiO2 systems

for results in $\Omega^{-1}cm^{-1}$:

$$\sigma_i = -3.34 + 6.64X_{CaO} + 6.5X_{MgO} + 8.06X_{MnO}. \quad (7)$$

Dukelow and Derge [2] provide results and discussion for the current efficiency of slags found in the $FeO-MnO-SiO_2$ system. It was found that current efficiency increases at higher MnO compositions and increases with corresponding increases in SiO_2 compositions.

Fontana et al. [10] investigated the diffusion and conduction properties of $CaO-SiO_2-MnO$ melts for various compositions and temperatures. They found that that the transport processes for the reaction

$$Mn^{2+} \rightarrow Mn^{3+} + 1e^- \quad (8)$$
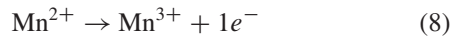
are controlled by the migration of Mn^{2+} as described by a modified Sand's Law solution to the Fick equations. They also found that in ternary $CaO-SiO_2-MnO$ melts, the silica has a more significant influence on both the diffusion coefficient D and the conductivity.

In recent work conducted in our laboratory [11, 12], the electrical conductivities of $FeO-SiO_2-CaO$ slags were examined as sums of ionic and electronic conductivities:

$$\sigma = \sigma_i + \sigma_e. \quad (9)$$

The ionic conductivity varied with oxygen potential due to the reaction

$$2Fe^{2+} + CO_2 = 2Fe^{3+} + CO + O^{2-}. \quad (10)$$
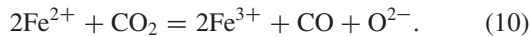
By varying the ratio CO_2/CO different oxidation states of the ions were attained. It was assumed that the ionic conductivity was negligibly affected by the higher oxidation species, Fe^{3+} due to the latter's formation of covalent anions (FeO_4^{5-} or $Fe_2O_5^{4-}$)[13]. By this means, a model for the ionic conductivity of the Fe^{2+} species was obtained as a function of Ca^{2+} and Fe^{2+} concentration and diffusivities

$$\sigma_i = \frac{4F^2}{RT}(C_{Ca^{2+}}D_{Ca^{2+}} + C_{Fe}D_{Fe^{2+}}(1-y)) \quad (11)$$

by application of the Nernst-Einstein equation, where C denotes concentration, D denotes the diffusion coefficient and y represents the ratio of Fe^{3+} to all iron species, Fe_{total}. The results from the study of Barati and Coley [11, 12] for ionic conductivity as a function of the Fe^{3+} fraction, y are presented in Figure 1 and exhibit the expected linear variation.

The electronic conductivity was found to vary according to $\sigma_e = by(1-y)$, and can be seen in Figure 2. The results obtained showed a distinct departure from the mechanism proposed by Mott [14], represented by in Equation 12:

$$\sigma_e = \upsilon_{ph}\frac{F^2}{RTN_ar}\exp(-2ar)\exp\left(\frac{-W}{RT}\right)y(1-y), \quad (12)$$
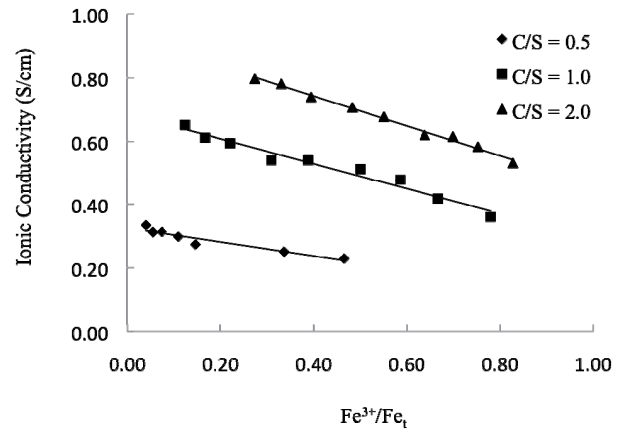
Figure 1. Variation of ionic conductivity at 1750K in the $FeO-SiO_2-CaO$ system with 30 mass% FeO, C/S= CaO / SiO_2 (data as reported in [12]).
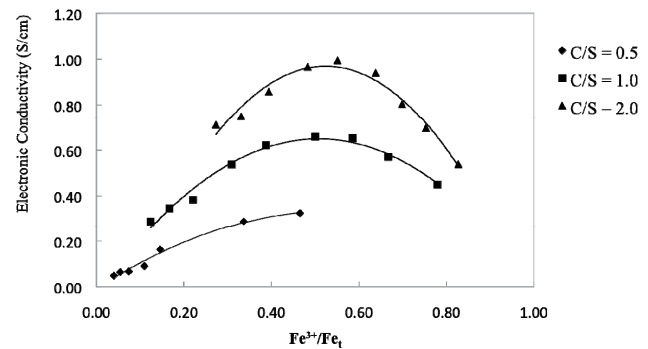

Figure 2. Variation of electronic conductivity at 1750K in the $FeO-SiO_2-CaO$ system (30 mass% FeO) C/S= CaO / SiO_2 (data as reported in [12]).
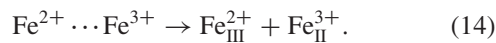
(with υ_{ph} being the phonon frequency, F being Faraday's constant, R being the gas constant, N_a being Avogadro's number, r being the mean hopping distance, W being the activation energy for the process and α being a quantum term representing rate of wave function decay).

Of particular note, Barati and Coley [12] found that the activation energy for electronic conduction was close to that for ionic conduction and decreased, as the total iron concentration increased, to become closer to that expected for small polaron hopping. They proposed that for hopping to occur, the ions involved in the process must be within a certain proximity and that the chances of two ions being within the required distance would increase with their concentration. Barati and Coley developed a "diffusion assisted hopping" model in an attempt to better describe the electronic conduction. Full details may be found in the original publications [11, 12], but the development of the model will be summarized here. First, the Fe^{2+} and Fe^{3+} species ap-

proach in a diffusion step:

$$\text{Fe}_{\text{II}}^{2+} + \text{Fe}_{\text{III}}^{3+} \frac{k_1}{K_1'} \text{Fe}_{\text{II}}^{2+} \cdots \text{Fe}_{\text{II}}^{3+}, \tag{13}$$
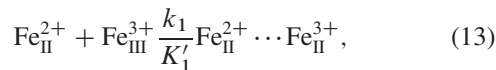
followed by the electron transfer:

$$\text{Fe}^{2+} \cdots \text{Fe}^{3+} \rightarrow \text{Fe}_{\text{III}}^{2+} + \text{Fe}_{\text{II}}^{3+}. \tag{14}$$

The result is

$$k_1 \left[\text{Fe}_{\text{II}}^{2+} \right] \left[\text{Fe}_{\text{III}}^{3+} \right] - \left(k_1' + k_2 \right) \left[\text{Fe}^{2+} + \cdots + \text{Fe}^{3+} \right] = 0 \tag{15}$$

under steady-state conditions. For $k_2 \ll k_1'$,

$$\upsilon_T = \frac{k_1 k_2}{k_1'} \left[\text{Fe}_{2+}^{\text{II}} \right] \left[\text{Fe}_{3+}^{\text{III}} \right], \tag{16}$$

where υ_T is the overall rate of charge transfer. The model for rate of encounter between ions was obtained using Fick's first law and steady-state assumptions. Use of Boltzmann statistics gives

$$\chi = 1 - \exp\left(-r^* \frac{EF}{RT} \right) \approx r^* \frac{EF}{RT} \tag{17}$$

for $EF > RT$, where χ is the probability that a charge transfer takes place upon the meeting of Fe^{2+} and Fe^{3+} species. Ions must diffuse from an initial distance r^0 from the stationary 3+ centre to the required distance for charge

Figure 3. Model schematic for diffusion assisted electron transfer as developed in the authors' previous study[12].

transfer, r^*. The schematic for the process is presented in Figure 3 for diffusion of B to A (B would be Fe^{2+} species and A would be Fe^{3+} species in this case).

The final result is the so-called diffusion-assisted charge transfer model:

$$\sigma_e = 4\pi N_a \frac{r^0 (r^*)^3}{r^0 - r^*} \frac{D_{\text{Fe}^{2+}} F^2}{RT} y(1 - y). \tag{18}$$

Excellent agreement was found between the obtained results and Equation 18. for a range of slag basicities.

Given the excellent accord obtained by the model for the consideration of $\text{FeO}_x\text{-SiO}_2\text{-CaO}$ slags with the experimental results, it is interesting to consider the transferability of the model in general. Specifically, can the diffusion-assisted charge transfer mechanism derived by Barati and Coley [12] be applied to different systems with multi-valent ions, to obtain reliable results? This question was the motivation for the present study. Similar experiments to those described in [11] were conducted in the $\text{MnO}_x\text{-SiO}_2\text{-CaO}$ system and the results analysed in terms of the diffusion assisted hopping model.

2 Experimental Procedure

The experimental procedure followed closely the procedure used in [11]. The central focus of the experimental procedure was the attainment of the electronic transference number, the ratio of electronic to total conductivity in the slag,

$$t_e = \frac{\sigma_e}{\sigma_t}. \tag{19}$$

Ionic conductivity is that resulting from the movement of ions themselves, whereas electronic conductivity results from a transfer of electrons between ions, rather than a direct movement of ions.

For measurement of the transference number, as in [11], the stepped potential chronoamperometry method was employed as introduced by Sadoway et al. [15] To determine the ionic and electronic conduction behaviour in BaO-TiO2 melts, Sadoway et al. applied a potential (in their case 0.80 mV) and observed the current response. Typical behaviour involves the immediate appearance of a peak, followed by a relaxation to a constant value of current. The immediate spike in current (at $t \rightarrow 0$) represents the combined ionic and electronic components. As $t \rightarrow \infty$, the current settles to a uniform value of, representing the contribution from electronic conduction only. This behaviour is to be expected, since ions become immobilized as $t \rightarrow \infty$ once they have moved to their preferred lowest-energy position. The only remaining conductance mechanism is the electronic component. This can be expressed in terms of
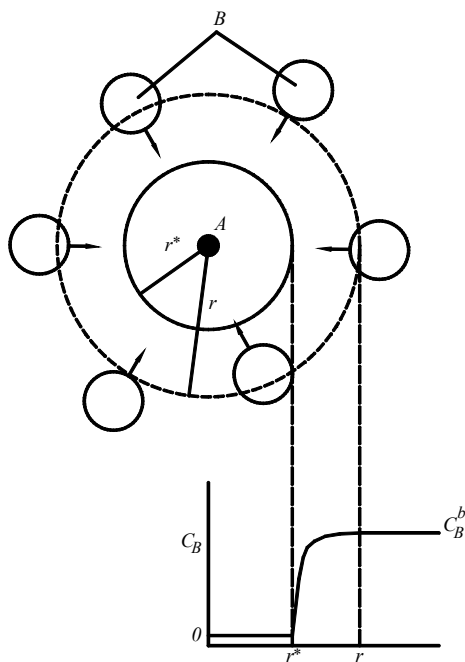
currents as shown in Equation 20.

$$t_e = \frac{i_e}{i_e + i_i}.$$ (20)

A typical current distribution obtained with the application of the potential can be seen in Figure 4, obtained during the MnO-CaO-SiO$_2$ experiments of this study. The current and the time are presented in arbitrary units, because the technique is only concerned with the ratio of the initial spike to the steady state value, therefore units are irrelevant.
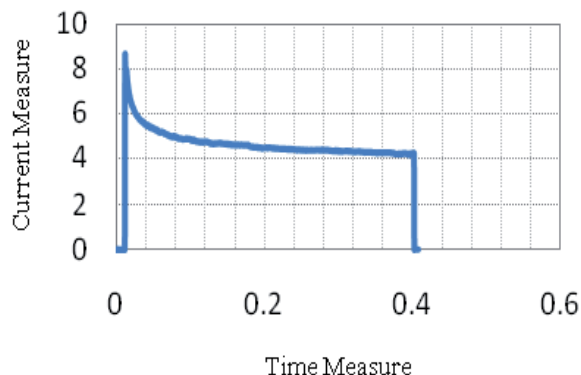
Figure 4. Typical response curve for SPC measurements.

Attempts were also made to measure the total conductivity using the procedure described in our previous work [11]. However dissolution of the electrode tips made these results unreliable. For that reason no data obtained in this study for total conductivities are presented. The measurement of transference numbers was not affected by electrode dissolution because it employed a comparative measurement over a very short timescale. For details of the experimental methods used to measure the total conductivity, the reader should consult reference [11].

The electrodes were composed of a Pt-Rh alloy (30 wt% Rh). This alloy was used, as described in [11] for its tensile strength, a useful attribute when entering the melt At the beginning of each experiment, resistances were taken at several frequencies to ensure independence of resistance of frequency (this was the case at each time). Measurements were typically taken at 20 kHz.

DC measurements were performed using a Model 273 potentiostat/galvanostat from Princeton Applied Research. Experiments were conducted at 0.2 V with the potential applied for several minutes. The device was controlled by Corr software for setting parameters and exporting data. Switching between the RCL meter and the potentiostat was facilitated by use of a simple switch mechanism. A four-electrode technique was used for the measurements.

A constant and controlled flow of gas over the slag sample was maintained throughout the course of the experiments. For the low Mn^{3+} experiments a constant gas flow

for the CO/CO$_2$ system was maintained at 500 cm^3/min for the higher Mn^{3+} range argon oxygen mixtures were employed. High purity argon was used overnight to ensure all oxygen was rmoved from the system. Before an experiment, the appropriate gas mixture was turned on and allowed to flow over the slag. After approximately 3 hours, an equilibrium was attained and the experiment could then proceed. This allowed control of the oxidation state distribution of the Mn ion species. Data reported by Sun and Jahanshahi [16] were fitted to the relation recommended in [17]. Gas flow was calibrated and controlled via mass controllers connected to PC software.

The transference number was determined by the stepped potential chronoamperometry method. Determination of the level of the top of the slag was determined by the location of a sudden and dramatic drop in resistance. The level of this drop was noted and used as the reference for depth measurements. The experiments were carried out at 1773 K, due to the wealth of diffusion and conductivity data available in the literature at this temperature. Resistances within the electrode probe were measured and subtracted from the measured resistance values. Two slag compositions were considered in this study, as shown in Table 1.

| Slag (Mass %)	MnO	CaO	SiO$_2$	C/S
A	30	23.3	46.7	0.5
B	30	33.8	36.2	0.93

Table 1. Slag compositions studied.

3 Results and Discussion

The results obtained for the transference numbers of the MnO-CaO-SiO$_2$ system are presented for the C/S ratio of 0.5 in Figure 5. Results for C/S of approximately 1.0 are presented in Figure 6. In both figures, the results from the FeO-CaO-SiO$_2$ melts are superimposed for comparison. It
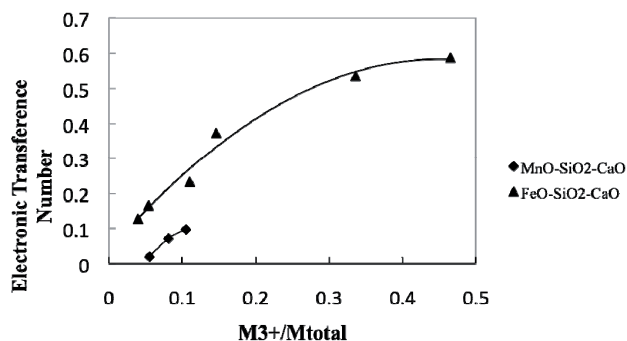
Figure 5. Transference number results at 1773 K for MnO-CaO-SiO$_2$ melts.
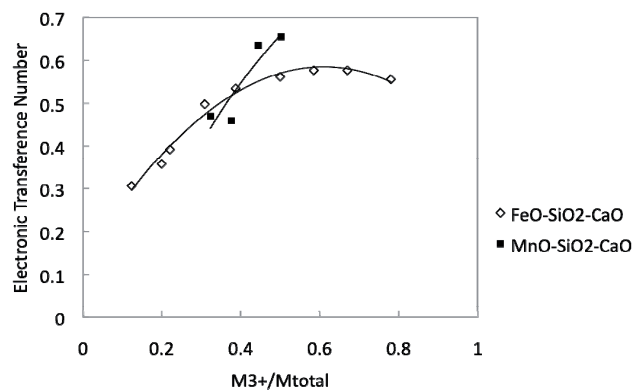
Figure 6. Transference number results obtained at 1773 K, for MnO-CaO-SiO$_2$ melts.

**Figure 7.** Model calculations plotted against measured results.

should be noted that in the case of the "C/S = 1.0" system, the MnO-CaO-SiO$_2$ system C/S ratio was in fact 0.93. It has been plotted with the FeO-CaO-SiO$_2$ results for C/S = 1 for comparison.

It is seen that for low ratios of M^{3+}/M_{total}, the electronic transference numbers in the MnO-CaO-SiO$_2$ system appear to be lower than those exhibited in the FeO-CaO-SiO$_2$ system, followed by a transition to higher values at higher ratios. Since measurements were taken at the very low range of M^{3+}/M_{total} and at values of around $M^{3+}/M_{total} = 0.4$–0.5, it is expected that measurements would have to be taken in the intermediate range to confirm this observation.

The applicability of the model derived by Barati and Coley [12] was tested against the transference number results by calculating σ_i and σ_e according to the model, followed by determination of the corresponding transference number. Parameters from the literature were used as input to the model. Values of D_{Mn}^{2+} obtained from Fontana et al. [10] were used, along with the value of D_{Ca}^{2+} obtained for the FeO-CaO-SiO$_2$ system, which was directly relevant to the system presently considered. With these inputs, only one parameter, the value r^* remained to be determined. This was done by selecting the value that gave the best fit to the current data. One value was assumed for the entire composition range. An excellent fit was obtained by selecting a realistic value close to that seen in the FeO-CaO-SiO$_2$ system. A plot of the measured versus model results is presented in Figure 7. The model using the value of r^* determined here shows excellent agreement when applied to total conductivity data measured by other workers. However the data used for comparison [8] was measured at low oxygen potentials where the electronic contribution would be negligible. It proved difficult to locate conductivity data for MnO-CaO-SiO$_2$ melts in the literature at the oxygen potentials required for any significant quantities of Mn^{3+} to be present. Consequently verification of the obtained results across the entire range of oxidation states was not possible.
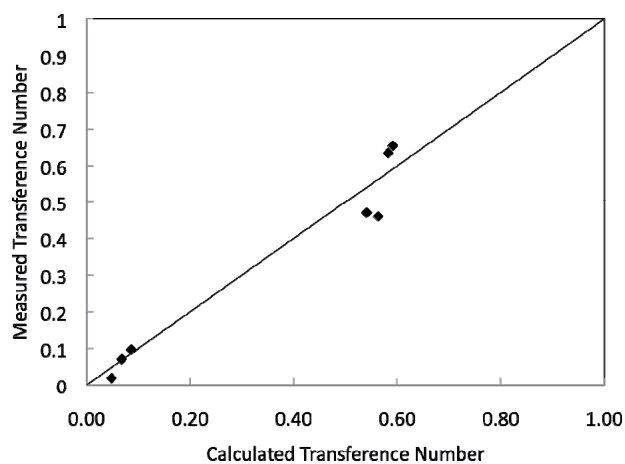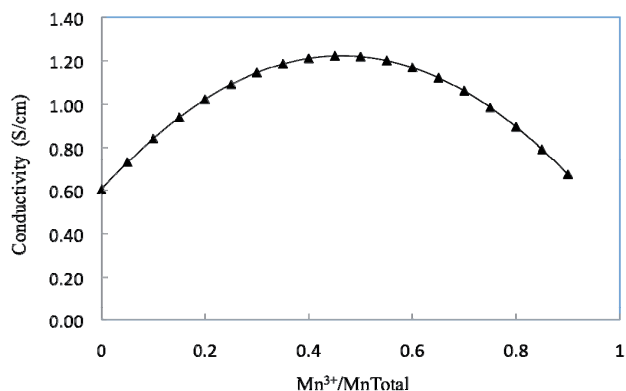
Figure 8. Calculated Total Conductivities as given by the model.

The results obtained from the previous study [12] applied to the FeO-CaO-SiO$_2$ showed excellent fit between the model and experimental results. Given the agreement at low oxygen potentials for the MnO-CaO-SiO$_2$ system, the excellent agreement in transference numbers and the fit in the iron system for all values of $3+/2+$, the model can be considered reliable for manganese slags. The behaviour of the calculated total conductivity for the system is given in Figure 8.

The value for the maximum distance between manganese $3+$ and $2+$ ions before charge transfer, r^* used in the model was 3.05 Angstrom for the MnO-CaO-SiO$_2$ system, whereas a value of 3.87 Angstrom for iron ions was found to

Fe Third Ionization Energy [18]	Mn Third Ionization Energy [18]
2957.3 kJ/mole	3248.3 kJ mol^{-1}

Table 2. Third Ionization Energies of Iron and Manganese

produce the excellent fit in the case of the : FeO-CaO-SiO_2 system. This variation is to be expected when considering the sizes of the third ionization energies (Table 2).

The higher third ionization energy of Mn requires a closer approach for electron transfer to occur. This observation is strong support for the reliability of the model as applied to this system.

4 Conclusions

(1) The diffusion assisted hopping model developed for FeO-CaO-SiO_2 has been shown to apply to the MnO-CaO-SiO_2 system, supporting the general applicability of this model to electronic conductivity in slags containing ions with multiple valence states.

(2) The maximum distance at which hopping can occur was found to be smaller for manganese than for iron. This is in keeping with the higher third ionization energies for manganese.

References

[1] W. R. Dickson and E. B. Dismukes, Trans. AIME, **224** (1962), 505–511.

[2] D. Dukelow and G. Derge, Trans. AIME, **218** (1960), 136–141.

[3] U. D. Pal, T. DebRoy and G. Simkovich, Metall. Trans. B, **16B** (1985), 77–82.

[4] E. T. Turkdogan, *Physicochemical Properties of Molten Slags and Glasses*, The Metals Society, 1983.

[5] E. A. Pastukhov, O. A. Esin and S. K. Chuchmarev, Sov. Electrochem., **2** (1966), 193–98.

[6] H. J. Engell and P. Vygen: Ber. Bunsengesellschaft, **72** (1968), 5–11.

[7] A. Fontana, K. Segers, K. Twite and R. Winand: TMS-AIME Papers Selection, paper no. A84-39 (1984)

[8] L. Segers, A. Fontana and R. Winand, Electrochimica Acta, **23** (1978), 1281–1286.

[9] Q. Jiao and N. J. Themelis, Metall. Trans. B, **19B** (1988), 133–140.

[10] A. Fontana, L. Segers and R. Winand, Can. Metall. Quart, **20**(2) (1980), 209–14.

[11] M. Barati and K. S. Coley, Metall. Mat. Trans. B, **37B** (2006), 41–49.

[12] M. Barati and K. S. Coley, Metall. Mat. Trans. B, **37B** (2006), 51–60.

[13] H. Flood and K. Grijotheim, J. Iron Steel Inst., **171** (1952), 64.

[14] N. F. Mott, J. Non-Cryst. Solids, **1** (1986), 1–17.

[15] N. A. Fried, K. G. Rhoads and D. R. Sadoway, Electrochimica Acta, **46** (2001), 3351–3358.

[16] S. Sun and S. Jahanshahi, Metall. and Mat. Trans. B, **31B** (2000), 937–943.

[17] L. Yang and G. Belton, Metall. and Mat. Trans. B,**29B** (1998), 837–845.

[18] D. R. Lide (editor), *CRC Handbook of Chemistry and Physics*, 80th ed., CRC Press (1999).